Pharm Res (2012) 29:1380–1391
DOI 10.1007/s11095-011-0647-7

RESEARCH PAPER

Local Gene Targeting and Cell Positioning Using Magnetic Nanoparticles and Magnetic Tips: Comparison of Mathematical Simulations with Experiments

Carsten Kilgus • Alexandra Heidsieck • Annika Ottersbach • Wilhelm Roell • Christina Trueck • Bernd K. Fleischmann • Bernhard Gleich • Philipp Sasse

Received: 5 August 2011 / Accepted: 5 December 2011 / Published online: 30 December 2011

ABSTRACT

Purpose Magnetic nanoparticles (MNPs) and magnets can be used to enhance gene transfer or cell attachment but gene or cell delivery to confined areas has not been addressed. We therefore searched for an optimal method to simulate and perform local gene targeting and cell delivery *in vitro*.

Methods Localized gene transfer or cell positioning was achieved using permanent magnets with newly designed soft iron tips and MNP/lentivirus complexes or MNP-loaded cells, respectively. Their distribution was simulated with a mathematical model calculating magnetic flux density gradients and particle trajectories.

Results Soft iron tips generated strong confined magnetic fields and could be reliably used for local (~500 μm diameter) gene targeting and positioning of bone marrow cells or cardiomyocytes. The calculated distribution of MNP/lentivirus complexes and MNP-loaded cells concurred very well with the experimental results of local gene expression and cell attachment, respectively.

Conclusion MNP-based gene targeting and cell positioning can be reliably performed *in vitro* using magnetic soft iron tips, and computer simulations are effective methods to predict and optimize experimental results.

KEY WORDS magnetic nanoparticles · localization · gene targeting · cell positioning · mathematical simulation

ABBREVIATIONS

BMC	bone marrow cells
GFP	green fluorescent protein
MNP	magnetic nanoparticle
MEA	microelectrode array

INTRODUCTION

Localized gene or drug delivery and cell positioning has great potential in biomedicine. It is obvious that site-restricted placement of drugs, genes and cells enhances the efficacy of the treatment and minimizes systemic side effects. One novel and promising approach to achieve site specific targeting *in vitro* and *in vivo* is to form complexes of the material with magnetic nanoparticles (MNPs). Due to their superparamagnetic properties, these particles experience force in inhomogeneous magnetic fields and hence can be manipulated through this field (1). Such external magnetic

Carsten Kilgus and Alexandra Heidsieck contributed equally to this manuscript.

C. Kilgus • A. Ottersbach • B. K. Fleischmann • P. Sasse (✉)
Institute of Physiology I, Life and Brain Center, University of Bonn
Sigmund-Freud-Str.25, 53127 Bonn, Germany
e-mail: philipp.sasse@uni-bonn.de

A. Heidsieck • B. Gleich (✉)
Zentralinstitut für Medizintechnik, Technische Universität München
Boltzmannstr. 11, 85748 Garching, Germany
e-mail: gleich@tum.de

W. Roell
Department of Cardiac Surgery, University of Bonn
Bonn, Germany

C. Trueck
Institute of Pharmacology and Toxicology, Biomedical Center
University of Bonn
Bonn, Germany

fields are not harmful for patients and could enable the site-specific positioning of MNPs in humans. This strategy has been proven to work for the enrichment of chemotherapeutic agents bound to ferrofluids (2,3), or for lung cancer therapy by inhalation of magnetic aerosol droplets (4,5).

Besides application in drug delivery systems, MNPs are widely used for enhanced gene expression *in vitro*, a technology called magnetofection (6). With this technique DNA (7), siRNA (8) or viruses (9,10) are coupled to MNPs to form complexes which are sedimented onto cells by an external magnetic field. Earlier studies have shown that this approach strongly enhances the efficiency of gene transfer because the diffusion limited adsorption step is reduced and the contact with the cells is enhanced, resulting in an accelerated cellular uptake of the complexes (9,11).

Although magnetofection has been established a few years ago, some issues have not been addressed to date. One of the major technical problems remaining is the design of a sufficiently strong magnetic gradient field that is concentrated on a small area, and enables highly efficient and focused transduction of very small areas *in vitro*, and within tissues or organs *in vivo*.

We (5,12) and other groups (13,14) have previously shown that the dynamic of magnetic particles can be simulated to predict the outcome of biological applications. Here we have modified these physical models to predict the positioning of MNP/lentivirus complexes and MNP-loaded cells *in vitro*. We calculated the movement of MNP complexes under the influence of different magnetic gradient fields for localized gene and cell delivery *in vitro*. This simulation allowed computing the required magnetic gradient field and designing the optimal magnetic source. Hence, we built different combinations of newly designed soft iron tips and NdFeB permanent magnets and used these for local transduction and cell positioning. We have compared the simulations with experimental data using transduction of cells with MNP/lentivirus complexes and positioning of MNP-loaded cells, and found good correlations. To demonstrate a useful application, we generated an electrically coupled monolayer using very low numbers of MNP-loaded, embryonic stem cell-derived cardiomyocytes that are difficult to be generated in high numbers.

MATERIALS AND METHODS

Numerical Methods for Particle and Cell Trajectories

The magnetic flux density resulting from the different geometries was calculated by means of numerical field calculations using the software Comsol Multiphysics 4.1 (Comsol Multiphysics GmbH, Goettingen, Germany). The relevant Maxwell equations were solved for a rotational symmetry and a triangular mesh with a typical number of elements of about 6,000 and an average mesh element quality of 0.97 to 0.98. The resulting data for the magnetic flux density field was exported into MATLAB® R2010b (MathWorks, Natick, MA, USA) on defined coordinates via the *LiveLink™ for Matlab* Module of Comsol Multiphysics. Discrete values were converted into continuous data with the help of spline interpolations.

The basic principle for the calculation of particle trajectories is based upon the balance between the magnetic and hydrodynamic force acting on a magnetic nanoparticle. Since there is no fluid flow present in the investigated setup, the hydrodynamic force consists solely of the Stoke's drag force, given by

$$\vec{F}_{hydro} = 3\pi\eta d\vec{v} \tag{1}$$

where d denotes the diameter of a spherical MNP/lentivirus complex or cell and η is the viscosity of the fluid, which was modeled as water (η=1 mPa·s). The velocity of the MNP/lentivirus complex or cell is described by v.

The magnetic force is generated by an external magnetic field and accelerates the particles in the direction of the magnetic field source. The force acting on a MNP/lentivirus complex or cell with the magnetic dipole moment μ within an external inhomogeneous static magnetic flux density field B is described by

$$\vec{F}_{mag} = \vec{\nabla}\left(\vec{\mu}\cdot\vec{B}\right) \tag{2}$$

Since the magnetic flux densities in the vicinity of the target region are above 150 mT and therefore large enough for the particles to be in saturation, we can assume the magnetic moment to be aligned to the external magnetic field and thus, the magnetic force can be simplified to

$$\vec{F}_{mag} = \mu\cdot\vec{\nabla}B \tag{3}$$

There are several minor forces which are disregarded in this work. Among those are diffusion and Brownian motion as well as gravity. Since they are several orders of magnitude smaller than the magnetic force, we neglected them for all further calculations (15).

Resulting from Eqs. 1 and 3, we can define the equation of motion for a MNP/lentivirus complex or cell as

$$m\dot{\vec{v}} = \mu\cdot\vec{\nabla}B - 3\pi\,\eta d\vec{v} \tag{4}$$

where m is the mass of the MNP/lentivirus complex or cell, respectively.

According to equation of motion (Eq. 4), the trajectories for N=10,000 particles were calculated separately using MATLAB. The sizes of the MNP/lentivirus complexes and cells were randomly generated according to their characteristic distributions (Fig. 1b). Their starting positions were uniformly distributed over the region of the fluid.

Because the particle masses are proportional to the volume, we have, as simplification, assumed that the distribution of the magnetic moment follows the distribution of the volume. The differential Eq. 4 was solved in MATLAB with an implicit Runge–Kutta algorithm (TR-BDF2). We assumed that once the particles reach the bottom, they adhere there (16) and particle movement was calculated for a maximum time of 30 min.

Analysis of Properties of Complexes and Loaded Cells

The size distribution of MNP/lentivirus complexes was determined by dynamic light scattering using a ZetaSizer (ZetaSizer Nano, Malvern Instruments Ltd, UK). The number-weighted diameter distribution was used for the calculations, where a refractive index of 2.42 (17) was used for the transformation. The size of the MNP-loaded cells was determined by evaluating microscopic images (Axiovert 200 and AxioVision 4.2, Carl Zeiss AG, Jena, Germany). The masses of the individual MNP/lentivirus complexes and cells are based on the amount of iron per MNP or cell, respectively. The magnetic moment of the MNP/lentivirus complexes and cells was determined by analyzing their movement in a well-defined magnetic field. In case of MNP/lentivirus complexes this was done by light absorption in a spectrophotometer (Specord 210, Analytik Jena, Jena, Germany) at 420 nm. Similar to the procedure described in ref. 8, we observed the change of light transmission over time and thereby were able to estimate the velocity of the MNP/lentivirus complexes. In the case of cells, the magnetic moment was determined by observing the cell movement via microscopy as previously described (18). In both cases, the magnetic moment was derived from the movement in the known magnetic gradient field, according to Eq. 4.

Design of Magnetic Tips for Localized Magnetic Flux Density Gradients

We explored different patterns of positioning MNP/lentivirus complexes or cells (a ring shape and spots with varying focus) and performed simulations to determine the appropriate magnetic gradient fields. To generate localized magnetic gradient fields we combined a permanent magnet and various soft iron tips. The permanent magnet is made of NdFeB with N50 magnetization, which corresponds to a remanent flux density of 1.41–1.45 T; it has a cylindrical geometry with a diameter of 30 mm and a height of 50 mm (STM-30x50-N, magnets4you GmbH, Lohr a. Main, Germany). On top of the magnet, we attached various tips made from soft iron (Armco Telar 57, AK Steel GmbH, Koeln, Germany). The advantage of soft iron compared to normal construction steel is its high saturation magnetization which is in the range of ~1.5 T.

MNP and Lentivirus Assembling and Local Transduction of HL-1 Cells

The HL-1 cardiomyocytes cell line which is derived from adult mouse atrial myocytes (19) was kindly provided by W. C. Claycomb, New Orleans, USA and cultured as previously described (19). HL-1 cells were plated on cover slips (diameter 25 mm) precoated with a 0.02% gelatine solution containing 5 µg/ml fibronectin (Sigma Aldrich, Muenchen, Germany). Local transduction experiments were performed one or two days after plating when cells were 70–80% confluent.

Throughout this study we have used the MNP SO-Mag5 because it is non-toxic in different endothelial and endothelial progenitor cell lines and has a high magnetic moment in MNP/lentivirus complexes (20).

SO-Mag5 MNPs are core-shell type nanoparticles that consist of a core of iron oxide and a surface coating of a silicon oxide with phosphonate groups. The iron oxide core was synthesized by precipitation of iron-hydroxide from aqueous solution of Fe(II)/Fe(III) salts and then transformation into magnetite in an oxygen-free atmosphere similar as reported before (21). The surface coating was performed by condensation of tetraethyl orthosilicate and 3-(trihydroxysilyl) propylmethylphosphonate which results in a silicon oxide layer with surface phosphonate groups as reported in detail by Mykhaylyk *et al.* (22). SO-Mag5 MNPs were synthesized and kindly provided by O. Mykhaylyk and C. Plank, Institute for Experimental Oncology and Therapy Research, Technische Universität München, Germany.

Lentiviral particles for the expression of the green fluorescence protein (GFP) under the ubiquitously active cytomegalovirus promoter were prepared as previously reported (23) and kindly provided by K. Zimmermann and A. Pfeifer, Department of Pharmacology and Toxicology, University Bonn.

MNP/lentivirus complexes were formed by incubation of lentiviral particles and SO-Mag5 for 20 min at room temperature in Hank's balanced salt solution supplied with $MgCl_2$ and $CaCl_2$ ($HBSS^{++}$; Invitrogen, Darmstadt, Germany) in a ratio of 200 fg iron/physical virus particle. In that range the maximal percentage of virus particles are bound to MNPs (20). MNP/lentivirus complexes had a stable electrokinetic potential of~-14 mV and an average hydrodynamic size of ~800 nm and these parameters remained stable over 1 h after complex formation (O. Mykhaylyk, personal communication).

For local transduction, cover slips with HL-1 cell layers were placed central onto a magnetic tip and MNP/lentivirus complexes were added in 500 µl $HBSS^{++}$ containing ~$5.75{\cdot}10^6$

virus particles and ~1.15 µg iron and horizontally shaken at a frequency of ~120/min. To prevent overgrowth, cell were mitotically inactivated with Mitomycin C (Sigma Aldrich) as previously reported (24). After three days of cultivation, cells expressed GFP and were fixated with 4% paraformaldehyde. Nuclear staining was performed with Hoechst 33342 (Sigma-Aldrich).

Local Positioning of Bone Marrow Cells

The investigation conforms with the Guide for the Care and Use of Laboratory Animals published by the US National Institutes of Health (NIH Publication No. 85-23, revised 1996) and approval was granted by local authorities. Bone marrow cells (BMC) were obtained from bones of the hind limbs of 12 weeks old male CD1 wild-type mice and cultivated as previously described (25). Five hours after isolation, BMC were loaded with MNPs by adding SO-Mag5 (20 pg iron/cell) over night. MNP-loaded cells did not aggregate and remained as single cells in suspension. For local cell positioning BMC (between 50,000 cells/ml and $1.5{\cdot}10^6$ cells/ml) were added to a 3 cm cell culture dish with a thin foil at the bottom (Lumox 35 mm, Sarstedt, Nuembrecht, Germany) and different magnetic tips were placed directly (~200 µm) underneath. The whole set-up was horizontally shaken for 16 min at 100/min.

Analysis of Localized Transduction and Cell Position

GFP and Hoechst fluorescence was recorded by generating overview images of the whole cell layer using a tiled-image recording system (10x objective, Axio Observer Z1, MosaiX module, Carl Zeiss AG). Brightfield images of cell distribution were recorded with a standard microscope (5x and 2.5x objective, Axiovert 200 M, Carl Zeiss AG) or a macroscope (MZ 16 F, Leica Microsystems, Wetzlar, Germany). The distribution of GFP or cell intensities were analyzed using ImageJ (U. S. National Institutes of Health, Bethesda, Maryland, USA) and the Radial Profile Plot Analysis plugin (see "Results").

Local Positioning of Purified Cardiomyocytes for Electrophysiological Recordings

Embryonic stem-cell derived purified cardiomyocytes were prepared as reported before (26) and loaded with SO-Mag5 at a ratio of 100 pg iron/cell over night. 5,000 cells were added in 800 µl to thin (180 µm) microelectrode arrays (MEAs) with 60 electrodes of 30 µm diameter and 200 µm interelectrode spacing (ThinMEA200/30iR-ITO, Multichannel Systems, Reutlingen, Germany) which were precoated with 10 µg/ml fibronectin. MEAs were subsequently placed on the 1 mm magnetic tip and horizontally shaken for 15 min at 120/min. After 24–48 h local field potentials were recorded with a MEA amplifier and the MC Rack software (Multichannel Systems) as reported earlier (27).

RESULTS

Design of Magnetic Tips

For local gene targeting or cell positioning we have designed a combination of several tips made of soft-iron on top of a cylindrical NdFeB permanent magnet (Fig. 1a). An iterative optimization process led to 4 different tip geometries (shapes are shown in Figs. 3a, g and 6a, g). The tips are denoted according to the diameter on their topmost point (0.2 mm, 1 mm and 3 mm). The diameter of the tip d_1 (0.2, 1 or 3 mm), the diameter of the magnet d_3 (30 mm) and the total height h_1+h_2 (35 mm) were held constant, whereas the values of the middle diameter d_2 and the heights (h_1 and h_2, see Fig. 1a) were subject to parameter runs to obtain the best magnetic gradient field with optimal magnitude and direction for the desired local particle accumulation. We have obtained the following values: 0.2 mm tip: h_1=17 mm, h_2=18 mm, d_2=10 mm; 1 mm tip: h_1=10 mm, h_2=25 mm, d_2=14 mm; 3 mm tip: h_1=15.4 mm, h_2=19.6 mm, d_2=14 mm.

Particle Properties

The magnetic force acting on a MNP/lentivirus complex or cell is proportional to its magnetic moment, which is in turn proportional to the volume. The hydrodynamic force that counteracts the magnetic force is proportional to the diameter. Therefore, particle properties like distribution of size and magnetic moment are important input parameters for the simulation. The size of MNP/lentivirus complexes was determined by dynamic light scattering and we obtained a lognormal distribution

$$d(x) = \frac{1}{\sqrt{2\pi}\sigma x}\exp\left(-\frac{(\ln x-\gamma)^2}{2\sigma^2}\right) \tag{5}$$

for the diameter (in nm) with σ=0.33 and γ=6.8 (Fig. 1b). The diameter (in nm) of MNP-loaded Bone marrow cells (BMC) was determined by evaluating microscopic images and we obtained a bimodal normal distribution

$$d(x) = \frac{1}{2\sqrt{2\pi}}\left(\frac{1}{\sigma_1}\exp\left(-\frac{(x-\gamma_1)^2}{2\sigma_1^2}\right)+\frac{1}{\sigma_2}\exp\left(-\frac{(x-\gamma_2)^2}{2\sigma_2^2}\right)\right) \tag{6}$$

with $\sigma_1=0.5{\cdot}10^3$, $\sigma_2=1.3{\cdot}10^3$, $\gamma_1=7{\cdot}10^3$, $\gamma_2=9{\cdot}10^3$ (Fig. 1b).

The magnetic moment of the particles and cells was determined by analyzing their movement in a well-defined magnetic field. In contrast to the methods described in ref. 8 and ref. 18, we have here taken the acceleration of MNP/

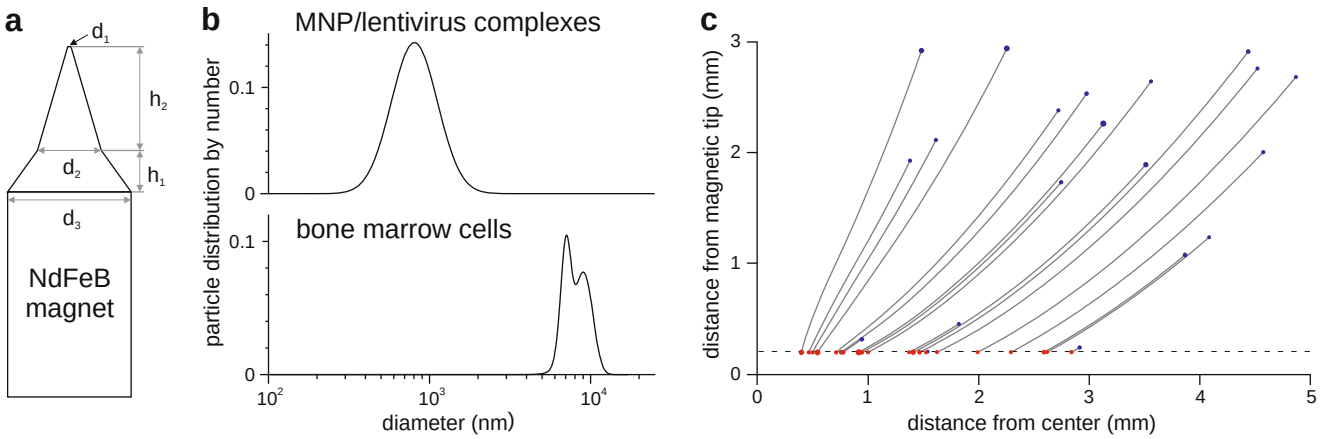

Fig. 1 (**a**) Dimensions of the permanent magnet and soft iron tips (for values see "Results"). (**b**) Lognormal distribution (according to Eq. 5) of MNP/lentivirus complexes diameter (*upper panel*) and bimodal normal distribution (according Eq. 6) of bone marrow cell diameter (*lower panel*). (**c**) Exemplary particle trajectories (*gray lines*) of MNP/lentivirus complexes from the simulation shown in Fig. 3h, I (dashed line: position of the culture dish; blue dots: starting positions; red dots: final positions; size of dots indicate particle size (not proportional)).

lentivirus complexes and cells into account. We obtained a magnetic moment to volume proportion

$$v = \frac{6\mu}{d^3\pi} \tag{7}$$

of ~$4{\cdot}10^3$ A/m and $8{\cdot}10^4$ A/m for MNP/lentivirus complexes and BMC, respectively. Hence, particles and cells differ not only in size, but also in magnetic moment.

Particle Trajectories

To determine the spatial distribution of gene or cell targeting experiments, we have simulated trajectories of 10,000 MNP/lentivirus complexes or MNP-loaded BMC according to Eq. 4 and analyzed the intersection of each trajectory with the bottom of the cell culture dish (example of 20 trajectories is shown in Fig. 1c). Simulations were carried out for a maximum time of motion of 30 min during which at least 98% of the particles have reached the bottom.

Transduction of HL-1 Cardiomyocytes with MNP/lentivirus Complexes with or without Magnetic Fields

To analyze local transduction we have used the cardiomyocyte cell HL-1 (19). Monolayers of coupled cardiomyocytes can be easily generated from these cells, which therefore represent a good model to investigate the origin of electrical activity and electrical conduction. For transduction, we generated MNP/lentivirus complexes by combining lentiviral particles that express the green fluorescent protein (GFP) under the control of the ubiquitous cytomegalovirus promoter with MNPs of the type SO-Mag5 (200 fg iron/physical virus particle). This specific MNP was chosen because SO-Mag5/lentivirus complexes are non-toxic for endothelial- (20) and HL-1 cells (data not shown), have a high magnetic moment, and are enhancing short-term transduction of cells (20). Transduction experiments were performed while shaking the cells horizontally for better distribution of MNP/lentivirus complexes. To exclude that shaking itself results in localized transduction, we have performed transduction experiments in the absence of a magnetic field as control and found that the GFP expression of the cells was scattered and non-localized (Fig. 2a). We have quantified the degree of localization of GFP transduction from independent experiments in form of distribution histograms. For this purpose we have measured the GFP intensity within shells of 250 µm distance (Fig. 2b), normalized it to the respective area of the shell to obtain the GFP density and normalized this value to the total GFP density of all shells. In full agreement with our

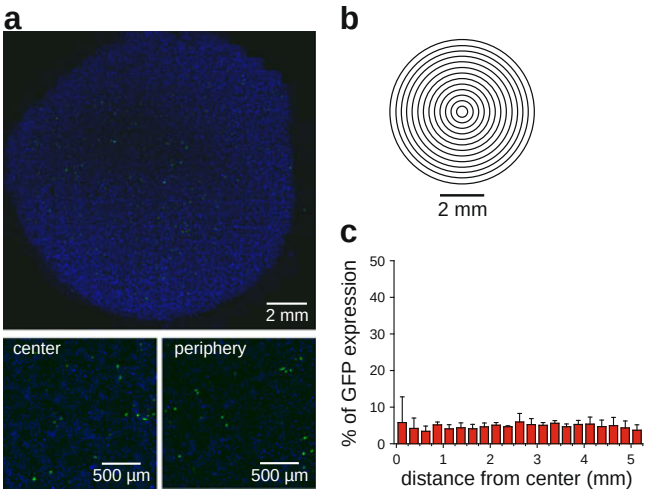

Fig. 2 Control experiments without magnets revealing homogeneous gene transfer. (**a**) Overview of GFP expression (*green*) after transduction of HL-1 cells with MNP/lentivirus complexes but without magnetic tips and enlargements from the center and periphery (nuclei shown in blue). (**b**) Illustration of the shells used for distribution analysis of GFP intensity, MNPs and cells in Figs. 2–6. (**c**) Statistical analysis of distribution of relative GFP expression density in individual shells without magnetic targeting ($n=6$).

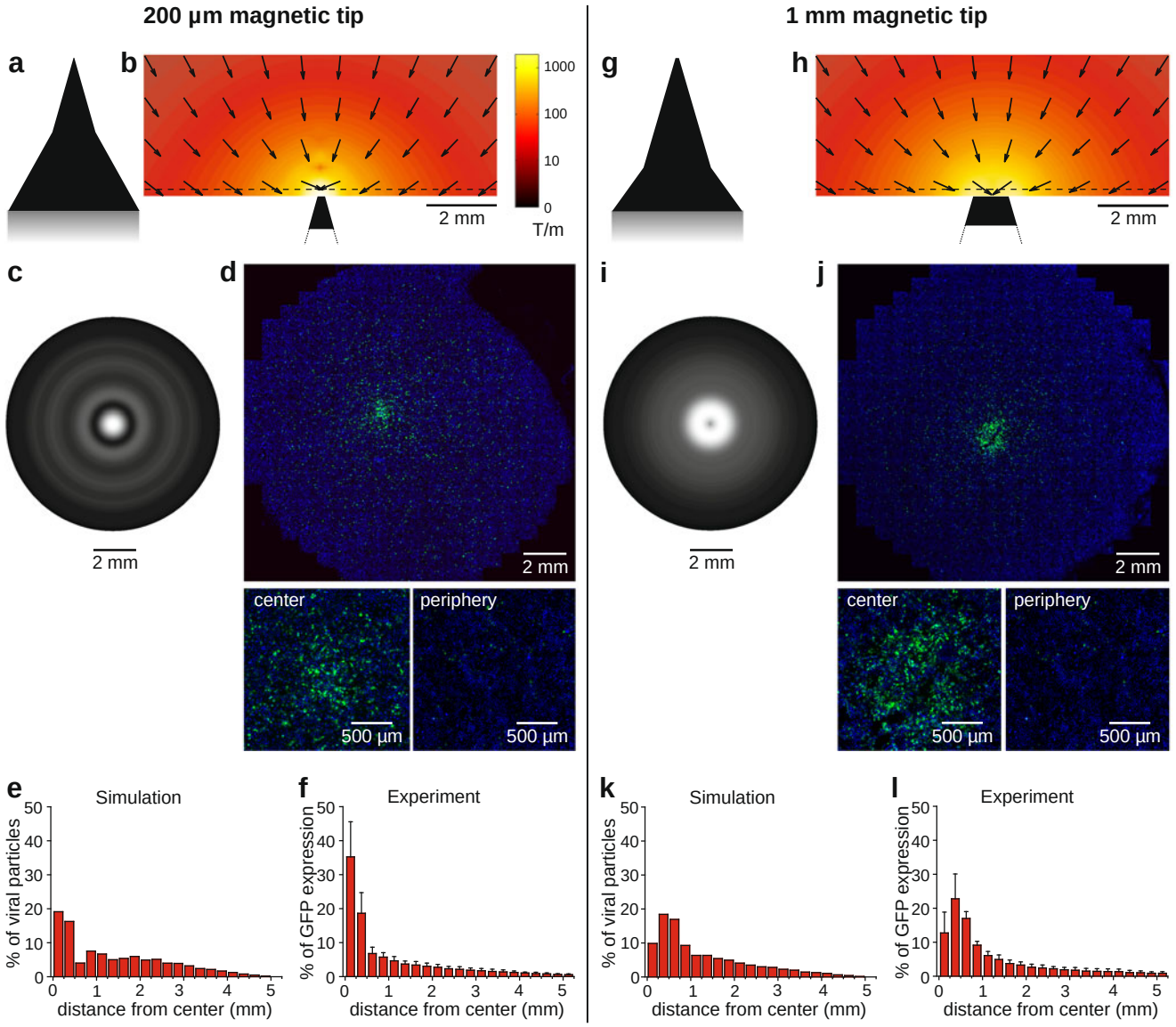

Fig. 3 Local transduction by 200 µm (**a**–**f**) and 1 mm (**g**–**l**) magnetic tips. (**a**, **g**) Shape of magnetic tips. (**b**, **h**) Absolute value (*color*) and direction (*arrows*) of magnetic flux density gradient in a cut through the symmetry plane (*dashed lines* indicate position of the culture dish). (**c**, **i**) Distribution of MNP/lentivirus complexes calculated from the simulations (intensity indicates amount of complexes). (**d**, **j**) Overview of GFP expression (*green*) of representative experiments after transduction of HL-1 cells with magnetic tips and enlargements from the center and periphery (nuclei shown in *blue*). (**e**, **k**) Distribution of simulated relative particle density in individual shells. (**f**, **l**) Distribution of relative GFP expression density in individual shells ((**f**) $n=6$; (**l**) $n=5$).

microscopic results, we found that the relative GFP density from experiments without magnetic field was very homogeneous in all shells (Fig. 2c) indicating that shaking does not result in localization.

Localized transduction of HL-1 cardiomyocytes was performed by placing a magnetic tip with 200 µm (Fig. 3a–f) or 1 mm (Fig. 3g–l) diameter below the cover slip and exposing the cells for 30 min to the MNP/lentivirus complexes. The magnetic tips produced a strong gradient of magnetic flux density which declined towards the periphery, and the direction of the gradient and therefore the direction of magnetic force on the MNPs was orientated towards the magnetic tips (Fig. 3b, h). Mathematical simulation of particle distribution showed that most of the MNP/lentivirus complexes remained within a small and focused area of ~1 mm diameter for the 200 µm tip (Fig. 3c) and of ~1.5 mm diameter for the 1 mm tip (Fig. 3i). These simulations are very well matched by the results of the transduction experiments, in which GFP expression was restricted to a central spot (Fig. 3d, j) of similar size as predicted by the simulations. In order to correlate the simulation with the experimental data, we generated distribution histograms of the simulated data using an identical method as for estimating the relative GFP density (see above). This analysis predicted that ~40% of particle density was found within the 500 µm around the center when using the 200 µm tip (Fig. 3e). This corresponded very well with the

experimental data that yielded ~55% of GFP density in this range (Fig. 3f). Similarly, the magnetic field of the 1 mm tip led to a localization to the first 750 µm, and ~50% of particle density in the simulation (Fig. 3k) and ~60% of GFP density in the experiment (Fig. 3l) was found in this range.

These results were obtained with cell layers placed 200 µm (thickness of glass cover slip) above the magnetic tip (dashed lines in Fig. 3b, h). We also assessed the impact of larger distances between the cells and the magnetic tips and have placed the cells 1 mm above the 1 mm magnetic tip (Fig. 4a, b). Both, simulations of particle distribution (Fig. 4c) and experimental data (Fig. 4d) showed consistently that localization was less confined and only 30% of particle (Fig. 4e) and GFP (Fig. 4f) density were found within 750 µm from the center.

Thus both magnetic tips could be reliably used for local transduction using MNP/lentivirus complexes, a larger distance between cells and magnetic tips resulted in a less confined localization and all these effects were perfectly predicted by mathematical simulations of particle distribution.

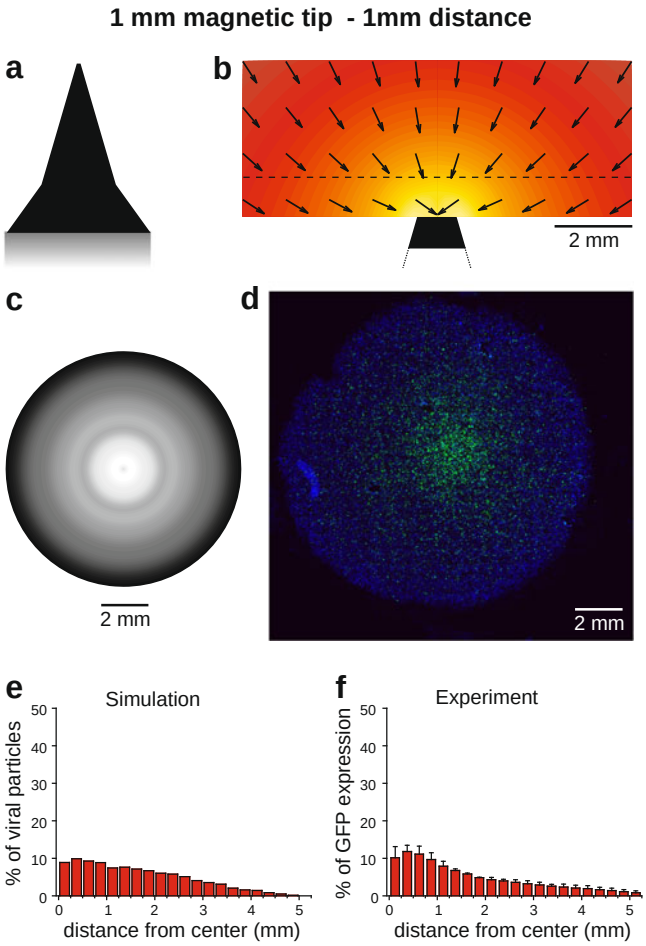

Fig. 4 Local transduction with cells positioned at 1 mm above (*dashed line* in B) the 1 mm magnetic tip. (**a**) Shape of magnetic tip. (**b**) Absolute value (*color*) and direction (*arrows*) of magnetic flux density gradient in a cut through the symmetry plane. (**c**) Distribution of MNP/lentivirus complexes calculated from the simulations (intensity indicates amount of complexes). (**d**) Overview of GFP expression (*green*) of a representative experiment (nuclei shown in *blue*). (**e**) Distribution of simulated relative particle density in individual shells. (**f**) Distribution of relative GFP expression density in individual shells ($n=5$).

Local Positioning of Bone Marrow Cells

Earlier work has proven that MNPs can be also used for cell accumulation onto magnetic stents (28) or within vessels (10). To analyze if our newly designed magnet tips could be employed for local cell enrichment, we have prepared BMC and loaded these with SO-Mag5 particles over night (20 pg iron/cell). We have chosen these cells because they are an autologous cell source, of small size passing through capillaries and could therefore be systemically applied for therapeutic purposes. Currently, autologous BMC are used for experimental therapies to treat heart failure (29). To analyze local cell enrichment, we used the 200 µm (Fig. 5a–d) and 1 mm (Fig. 5e–h) magnetic tips with identical geometries and gradients of magnetic flux densities as described above (Fig. 3a, b and Fig. 3g, h, respectively). For the simulation of cell distribution, the different physical characteristics (mass, size and ratio of magnetic moment to volume) of the MNP-loaded BMC were taken into account. Although these physical characteristics of cells and MNP/lentivirus complexes clearly differ (Fig. 1b), the simulations yielded a very similar distribution pattern (compare Fig. 3c with Fig. 5a and Fig. 3i with Fig. 5e). Using the 200 µm tip for local cell positioning, the MNP-loaded BMC were localized in a very confined spot of 500 µm diameter (Fig. 5b) and consequently ~90% cell density was found within 250 µm from the center (Fig. 5d). This is a much better localization than predicted by the simulation (Fig. 5a) which yielded only about 30% of cell density within this distance (Fig. 5c). Interestingly, the 1 mm tip lead to a cell deposition in a ring shaped area of 1 mm diameter but with a central spot without cells (Fig. 5f). The statistical analysis of these experiments revealed that the highest (~65%) cell density was found in the region between 250 and 750 µm distance from the center and these results were very similar to the simulation (Fig. 5g, h).

The different patterns of attracted cells are due to the fact that the gradient of the magnetic flux density and thus the force acting on the particles or cells is highest at the edges of the soft iron tip. The magnetic field lines are guided within the geometry of the tip, due to its ferromagnetic material properties. By narrowing the tip, the density of magnetic field lines and thus the magnetic flux density increases. Hence, a high gradient on top of the magnet tip occurs and is highest at the edges of the tip. To analyze the influence of these edges in more detail, we designed two differently shaped magnetic tips with 3 mm diameters and performed again simulations and experiments of cell positioning. The flat tip (Fig. 6a, b) lead to a positioning of cells within a circle of ~3 mm diameter in both

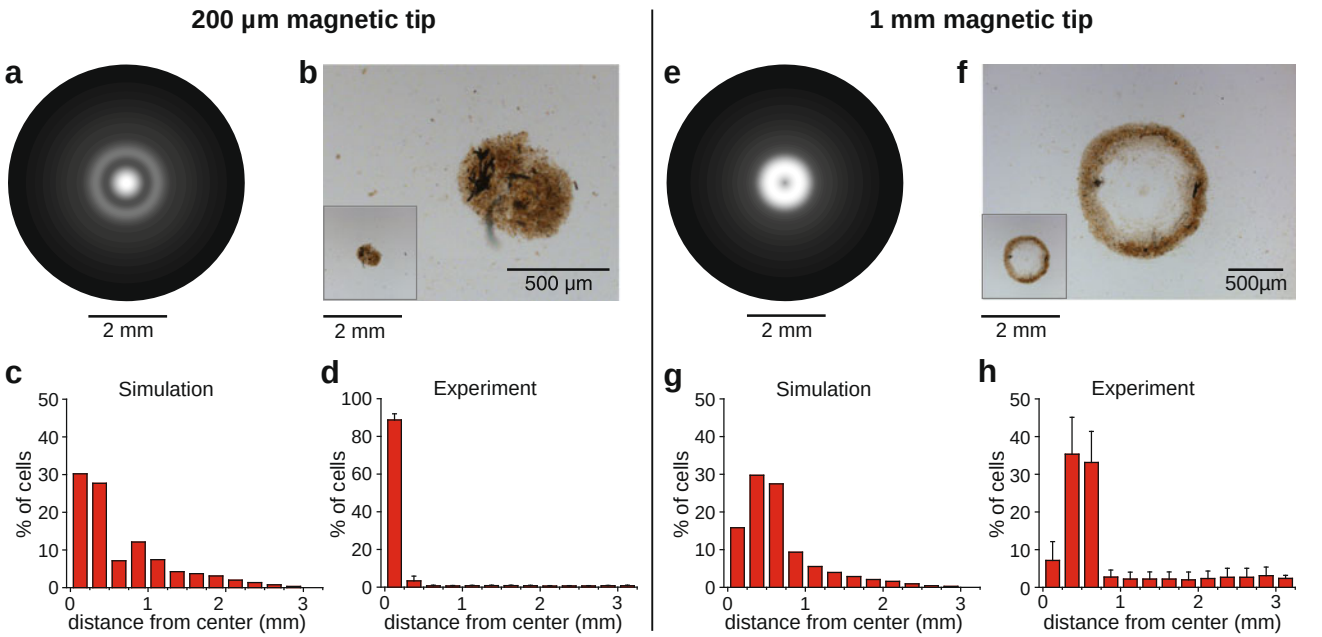

Fig. 5 Local cell positioning of BMCs by 200 μm (**a**–**d**) and 1 mm (**e**–**h**) magnetic tips. (**a**, **e**) Distribution of cells calculated from the simulations (intensity indicates amount of cells). (**b**, **f**) Local cell accumulation of representative experiments (for comparison, inserts are shown with same magnification than (**a**, **e**)). (**c**, **g**) Distribution of simulated cell density in individual shells. (**d**, **h**) Distribution of relative cell density in individual shells analyzed form experiments ((**d**) n=4; (**h**) n=4).

the simulation and experiments (Fig. 6c, d) which was also confirmed in the statistical analysis (Fig. 6e, f).

In order to generate a more homogeneous cell distribution and not only a ring structure we have designed a 3 mm tip with a slimmer geometry and rounded edges (Fig. 6g, h). In this case the mathematical optimization process did not only include the magnitude of the magnetic flux density gradient but also the direction of the magnetic force. The angle of the magnetic force vector with the cell culture dish was optimized for smaller perpendicular components at the edges. As a result, more horizontal movement should be achieved before the particles reach the bottom and adhere. We have obtained the following values: h_1: 15 mm, h_2: 5 mm, d_2: 3 mm, r_2: 1 mm (Fig. 6g, h). Simulation of cell localization using this tip predicted a more homogeneous ring shape with a diameter of 2 mm and with a very small cell-free area in the center (Fig. 6i, k). However, the experimental data did not reproduce these simulation results and cells were still localized in a ring shape with a large central cell-free area (Fig. 6j, l).

Local Positioning of Cardiomyocytes for Electrophysiological Analysis

The electrophysiological function of single cardiomyocytes differs from that within an electrical syncytium like the heart. To mimic such an electrical syncytium *in vitro*, we have tried to generate monolayers of electrically coupled cardiomyocytes on top of microelectrode arrays (MEAs). MEAs are cell culture plates with ~300 mm^2 total area and 60 electrodes in the center covering a square area of 2 mm^2 (Fig. 7a). With these devices field potentials as well as conduction velocities can be measured and can be therefore used to investigate diseased-specific cardiomyocytes (30) and to perform drug testing. The generation of monolayers with biologically relevant cardiomyocytes such as pluripotent cell-derived cardiomyocytes is very difficult because such cells do not proliferate and obtaining large enough numbers is labor intense and costly. Therefore, we sought to generate monolayers with very low numbers of cardiomyocytes (~5,000) taking advantage of magnetic cell positioning. We have used purified embryonic stem cell-derived cardiomyocytes (26) and loaded these with SO-Mag5 particles over night (100 pg iron/cell). To prove functional coupling we recorded the local electrical activity of cardiomyocytes with MEAs. As controls, MNP-loaded cardiomyocytes were added to MEAs without magnetic positioning, which resulted in a scattered attachment of cells (Fig. 7a) and only few or no electrodes showed electrical activity (Fig. 7b). In contrast, when the same number of cells were localized to the electrode area of MEAs (Fig. 7c) using the 1 mm magnetic tip, synchronous electrical activity (Fig. 7d) was observed proving generation of a functional syncytium of electrically coupled cardiomyocytes.

DISCUSSION

We have shown that localized gene delivery and cell positioning can be effectively performed by combining MNP/lentivirus complexes or MNP-loaded cells with confined strong magnetic fields generated by specially designed soft iron

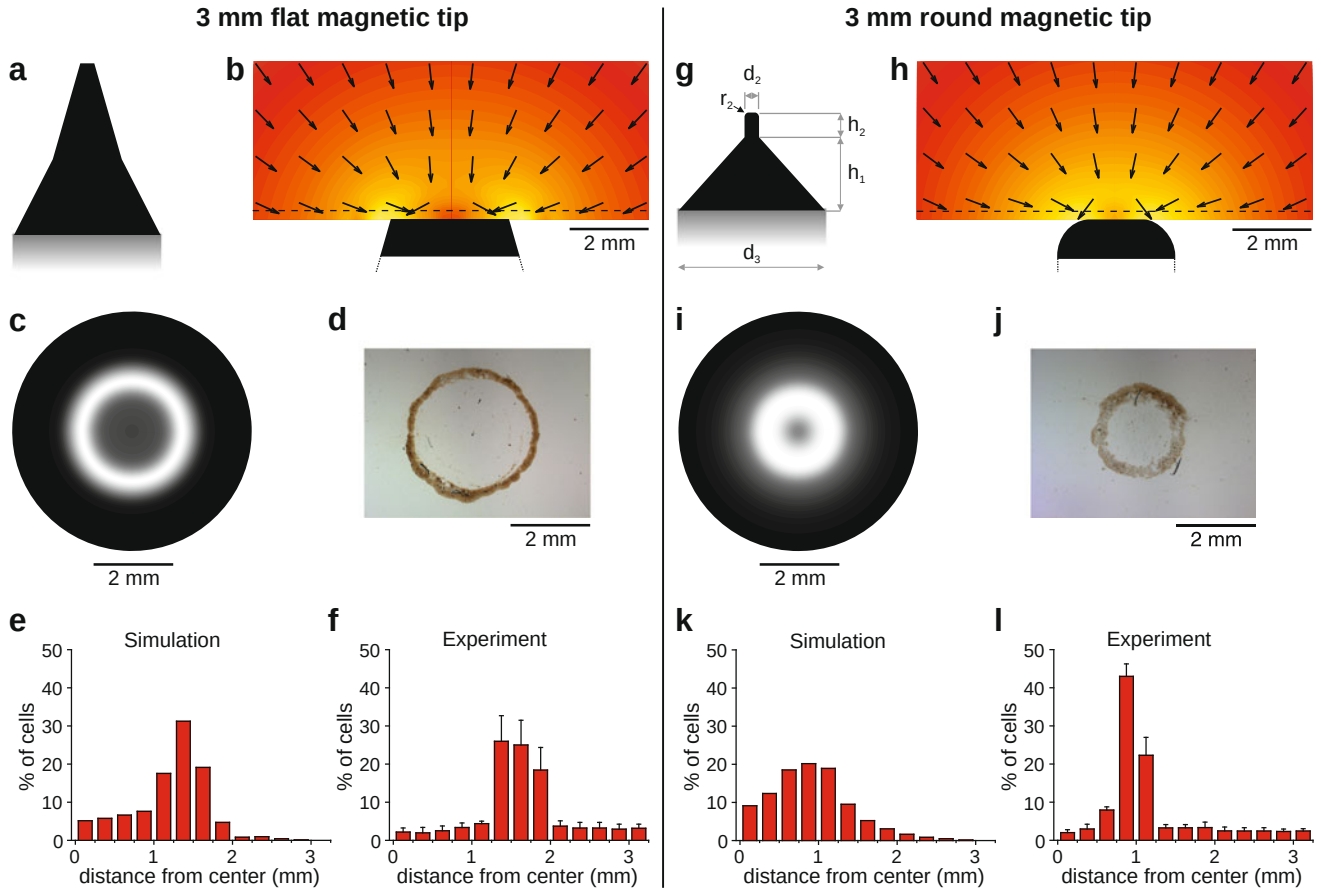

Fig. 6 Local cell positioning of BMCs by 3 mm magnetic tips with flat (**a**–**f**) and round (**g**–**l**) design. (**a**, **g**) Shape of magnetic tips. (**b**, **h**) Absolute value (*color*) and direction (*arrows*) of magnetic flux density gradient in a cut through the symmetry plane (*dashed lines* indicate position of the culture dish). (**c**, **i**) Distribution of cells calculated from the simulations (intensity indicates amount of cells). (**d**, **j**) Local cell accumulation of representative experiments. (**e**, **k**) Distribution of simulated cell density in individual shells. (**f**, **l**) Distribution of relative cell density in individual shells analyzed form experiments ((**f**) $n=4$; (**l**) $n=4$).

tips and permanent magnets. We performed mathematical simulations by calculating the trajectories of particles in the magnetic field and took into account the physical properties of MNP/lentivirus complexes or MNP-loaded cells. We showed that in most cases these predictions concur well with the outcome of experiments.

The use of MNP/lentivirus complexes for magnetofection (6–11) and the positioning of MNP-loaded cells (10,28) has been previously reported, but localization of gene transfer to a confined area below 5 mm (31) has not been studied in detail. The main difficulty for studying this issue is to achieve large enough forces with very small magnets. We therefore searched for alternatives to generate magnetic forces focused on small target regions, and developed different soft iron tips attached to a larger permanent magnet.

In order to simulate the distribution of MNP/lentivirus complexes or MNP-loaded cells, we modified an established magnetic drug targeting model (12) to determine local accumulation of magnetic particles and cells in dependence of the magnetic flux density and the tip geometry. In contrast to other work in this field (32,33), in which such problems were solved analytically or as a non-accelerated movement, we included physical particle and cell properties and approximated the experiments by simulating a high number of particles to reduce statistical fluctuations. Hereby, we were able to include the whole distribution of MNP/lentivirus complexes and cell sizes, instead of using only a mean diameter. Although we did not include contributions of minor forces and interactions between particles or cells in our simulations, the results of the simulation are in good agreement with the experimental results.

The discrepancies between simulations and experiments in cell positioning using the 200 µm magnetic tip (Fig. 5c, d), or the 3 mm round magnetic tip (Fig. 6k, l) could be explained by horizontal shaking during the experiments. The influence of lateral movement of cells and fluids was neglected in our calculations, but could well influence the final attachment of cells, especially in the region with low magnetic forces. Additionally, we did not account for the influence of already adherent cells, because the trajectories and final positions were calculated for each cell individually. Attached cells could obstruct the movement of other cells by

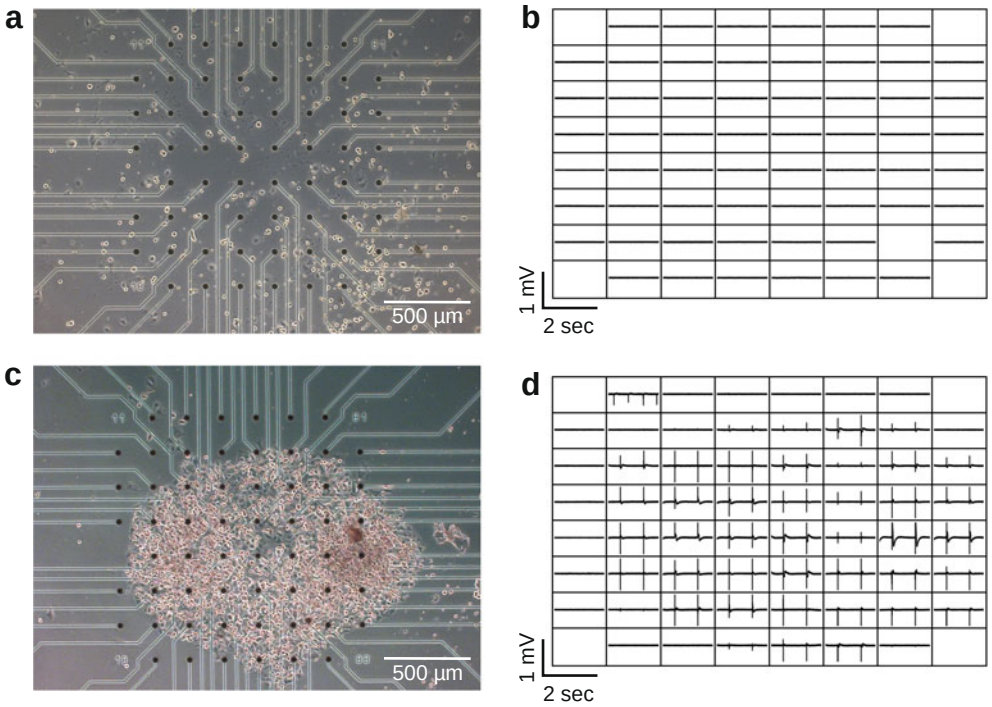

Fig. 7 (**a**, **b**) Control experiment of plating MNP-loaded cardiomyocytes on a MEA without magnetic tips (**a**) and field potential recordings (**b**). (**c**, **d**) Local positioning of MNP-loaded cardiomyocytes using the 1 mm magnetic tip below the electrode area (**c**) and field potential recordings (**d**).

building a "wall" of cells preventing other cells to reach the center of the magnetic tip (compare Fig. 6k with Fig. 6l)

In contrast to a distance of 200 µm between cells and magnetic tips which lead to good local positioning, we found that a distance of 1 mm results in less localization of transduction (Fig. 4). This is because it is not possible to generate a maximum of magnetic flux density at a point distant from the magnet. However, it might be possible to partially circumvent this problem, e.g. by using a second counterpole on top of the set-up. This does not lead to larger magnetic flux density gradients, but reduces the radial component of the magnetic flux density gradient which is generated by the magnetic tips.

Localized gene or cell targeting *in vitro* will be useful in the future to investigate biological processes in the culture dish that involve regional differences in gene expression or local activity of cells in microenvironments. We here have shown that a cell line of cardiomyocytes can be locally transduced with MNP/lentivirus complexes. This could be used to identify the spatial and genetic requirements for building an optimal pacemaker in the culture dish by a series of local transductions with multiple shapes of magnetic fields and expression of different pacemaker genes.

MNP-based cell positioning was used before for generation of a multilayered cardiomyocyte sheet (34,35). We have followed this idea and proved that a functional syncytium of electrically coupled cardiomyocytes can be generated *in vitro* with very few MNP-loaded cardiomyocytes and the newly designed 1 mm magnetic tip. This technology could help to investigate the function and therapy of disease-specific cardiomyocytes (30), whose generation in large numbers is costly and time-consuming.

Besides the *in vitro* applications which we have explored in the present work, the combined use of MNPs and magnetic tips might be useful for localized gene therapy *in vivo*. For this purpose it is mandatory that MNP/lentivirus complexes are I) physically stable in the blood, II) small enough to pass the capillary bed, III) not unspecifically absorbed by endothelial cells and IV) captured by strong localized magnetic fields within the tissue. Magnetic targeting of MNP/lentivirus complexes within the blood flow appears in principle possible, because the magnetic force is proportional to the volume of the complexes and therefore exceeds counteracting hydrodynamic forces, which are only proportional to the diameter. In addition, the targeting efficacy in biological flows *in vivo* is determined by several other aspects, such as vessel dilatation or non-newtonian flow properties (see discussion in ref. 12). In general, the size of magnetic force is determined by the magnetic moment of the MNPs and the magnitude of the magnetic gradient.

The size of the magnetic moment depends on the core material and core diameter of MNPs and the size of MNP/lentivirus complexes. Magnetite, which is used in the core of SO-Mag5 has the highest intrinsic magnetic moment among superparamagnetic materials. Increasing the core diameter of MNP to achieve higher magnetic moments is a limited process, because this will eventually lead to a ferromagnetic behavior with aggregation of MNPs in magnetic fields. Also increasing the size of MNP/lentivirus complexes is limited and might lead to thrombosis of capillaries. The complexes that we obtained using SO-Mag5 and lentiviruses were below 1 µm in diameter

(20), and should therefore pass capillaries without the risk of thrombosis.

To obtain large magnetic gradients, previous studies in small animals have used large permanent magnets that, however, resulted in little localization of gene expression (10,31). Our newly designed magnetic tips that generate very strong and localized magnetic field gradients at the tip, might be useful for more confined targeting of MNP/lentivirus complexes to restricted regions within organs. Because the magnetic gradient declines rapidly with distance between magnet and target, MNP-aided gene transfer will only be feasible close to the body surface. For deeper applications in larger animals or humans, implantation of magnetic micro arrays (14) or non-magnetic devices that can be magnetized by external magnets and generate high and local field gradients (36) might be much better suited. In addition, the imaging gradients of magnetic resonance imaging systems were used before for cell guiding *in vitro* (37) and this technology could be also used for magnetic cell or gene targeting inside the body.

Further optimization of MNPs and magnetic fields are required before reliable and efficient gene or cell targeting can be performed in humans.

CONCLUSION

We have shown that localized gene targeting or cell positioning can be reliably performed *in vitro* using magnetic tips and MNP/lentivirus complexes or MNP-loaded cells, respectively. The established new simulation algorithm was useful to predict the outcome of experiments and to optimize magnetic field gradients. These new tools will not only enable the investigation of localization effects on biological processes or the bioengineering of tissues *in vitro* but could also be used in the future to optimize cell and gene targeting *in vivo*.

ACKNOWLEDGMENTS & DISCLOSURES

We thank O. Mykhaylyk and C. Plank, Institute for Experimental Oncology and Therapy Research, Technische Universitaet Muenchen, Germany for providing the SO-Mag5 MNP, K. Zimmermann and A. Pfeifer, Institute of Pharmacology and Toxicology, University of Bonn, Germany for providing the cytomegalovirus-GFP lentivirus, W. C. Claycomb, New Orleans, USA for providing the HL-1 cell line, and K. Granitza and the machine shop of the Institute of Physiology, University Bonn for machining the soft iron tips.

This work was supported by grants of the German Research Foundation within the DFG Research Unit 917 "Nanoparticle-based targeting of gene- and cell-based therapies."

REFERENCES

1. Krishnan KM. Biomedical nanomagnetics: a spin through possibilities in imaging, diagnostics, and therapy. IEEE Trans Magn. 2010;46(7):2523–58.
2. Lübbe AS, Alexiou C, Bergemann C. Clinical applications of magnetic drug targeting. J Surg Res. 2001;95(2):200–6.
3. Alexiou C, Jurgons R, Schmid RJ, Bergemann C, Henke J, Erhardt W, *et al.* Magnetic drug targeting–biodistribution of the magnetic carrier and the chemotherapeutic agent mitoxantrone after locoregional cancer treatment. J Drug Target. 2003;11(3):139–49.
4. Ally J, Martin B, Khamesee MB, Roa W, Amirfazli A. Magnetic targeting of aerosol particles for cancer therapy. J Magn Magn Mater. 2005;293(1):442–9.
5. Dames P, Gleich B, Flemmer A, Hajek K, Seidl N, Wiekhorst F, *et al.* Targeted delivery of magnetic aerosol droplets to the lung. Nat Nanotechnol. 2007;2(8):495–9.
6. Plank C, Schillinger U, Scherer F, Bergemann C, Remy JS, Krotz F, *et al.* The magnetofection method: using magnetic force to enhance gene delivery. Biol Chem. 2003;384(5):737–47.
7. Al-Deen FN, Ho J, Selomulya C, Ma C, Coppel R. Superparamagnetic nanoparticles for effective delivery of malaria DNA vaccine. Langmuir. 2011;27(7):3703–12.
8. Mykhaylyk O, Zelphati O, Rosenecker J, Plank C. siRNA delivery by magnetofection. Curr Opin Mol Ther. 2008;10(5):493–505.
9. Scherer F, Anton M, Schillinger U, Henke J, Bergemann C, Kruger A, *et al.* Magnetofection: enhancing and targeting gene delivery by magnetic force *in vitro* and *in vivo*. Gene Ther. 2002;9(2):102–9.
10. Hofmann A, Wenzel D, Becher UM, Freitag DF, Klein AM, Eberbeck D, *et al.* Combined targeting of lentiviral vectors and positioning of transduced cells by magnetic nanoparticles. Proc Natl Acad Sci U S A. 2009;106(1):44–9.
11. Haim H, Steiner I, Panet A. Synchronized infection of cell cultures by magnetically controlled virus. J Virol. 2005;79(1):622–5.
12. Gleich B, Weyh T, Wolf B. Magnetic drug targeting: an analytical model for the influence of blood properties on particle trajectories. Applied Rheology 2008;18(5).
13. Babinec P, Krafcik A, Babincova M, Rosenecker J. Dynamics of magnetic particles in cylindrical Halbach array: implications for magnetic cell separation and drug targeting. Med Biol Eng Comput. 2010;48(8):745–53.
14. Krafcik A, Babinec P, Babincova M. Feasibility of subcutaneously implanted magnetic microarrays for site specific drug and gene targeting. J Eng Sci Tech Rev. 2010;3(1):53–7.
15. Gleich B, Hellwig N, Bridell H, Jurgons R, Seliger C, Alexiou C, *et al.* Design and evaluation of magnetic fields for nanoparticle drug targeting in cancer. IEEE Trans Nanotechnol. 2007;6(2):164–70.
16. Sharma MM, Chamoun H, Sarma DSHS, Schechter RS. Factors controlling the hydrodynamic detachment of particles from surfaces. J Colloid Interface Sci. 1992;149(1):121–34.
17. Cornell U, Schwertmann U. The Iron Oxides. Weinheim, Germany: VCH Publishing Group; 1996.
18. Hafeli UO, Lobedann MA, Steingroewer J, Moore LR, Riffle J. Optical method for measurement of magnetophoretic mobility of individual magnetic microspheres in defined magnetic field. J Magn Magn Mater. 2005;293(1):224–39.
19. Claycomb WC, Lanson NA, Stallworth BS, Egeland DB, Delcarpio JB, Bahinski A, *et al.* HL-1 cells: A cardiac muscle cell line that contracts and retains phenotypic characteristics of the adult cardiomyocyte. Proc Natl Acad Sci U S A. 1998;95(6):2979–84.
20. Trueck C, Zimmermann K, Mykhaylyk O, Anton M, Vosen S, Wenzel D, *et al.* Optimization of magnetic nanoparticles assisted

lentiviral gene transfer. Pharm Res. 2011. doi:10.1007/s11095-011-0660-x.
21. Mykhaylyk O, Sanchez-Antequera Y, Vlaskou D, Hammerschmid E, Anton M, Zelphati O, *et al.* Liposomal magnetofection. Meth Mol Biol. 2010;605:487–525.
22. Mykhaylyk O, Sobisch T, Almstätter I, Sanchez-Antequera Y, Brandt S, Anton M, *et al.* Silica-iron oxide magnetic nanoparticles modified for gene delivery. A search for optimum and quantitative criteria. Pharm Res. 2011. doi:10.1007/s11095-011-0661-9.
23. Pfeifer A, Hofmann A. Lentiviral transgenesis. Meth Mol Biol. 2009;530:391–405.
24. Becher UM, Breitbach M, Sasse P, Garbe S, van der Ven PF, Furst DO, *et al.* Enrichment and terminal differentiation of striated muscle progenitors *in vitro*. Exp Cell Res. 2009;315(16):2741–51.
25. Breitbach M, Bostani T, Roell W, Xia Y, Dewald O, Nygren JM, *et al.* Potential risks of bone marrow cell transplantation into infarcted hearts. Blood. 2007;110(4):1362–9.
26. Kolossov E, Bostani T, Roell W, Breitbach M, Pillekamp F, Nygren JM, *et al.* Engraftment of engineered ES cell-derived cardiomyocytes but not BM cells restores contractile function to the infarcted myocardium. J Exp Med. 2006;203(10):2315–27.
27. Bruegmann T, Malan D, Hesse M, Beiert T, Fuegemann CJ, Fleischmann BK, *et al.* Optogenetic control of heart muscle in vitro and *in vivo*. Nat Methods. 2010;7(11):897–900.
28. Pislaru SV, Harbuzariu A, Gulati R, Witt T, Sandhu NP, Simari RD, *et al.* Magnetically targeted endothelial cell localization in stented vessels. J Am Coll Cardiol. 2006;48(9):1839–45.
29. Murry CE, Field LJ, Menasche P. Cell-based cardiac repair: reflections at the 10-year point. Circulation. 2005;112(20):3174–83.
30. Malan D, Friedrichs S, Fleischmann BK, Sasse P. Cardiomyocytes Obtained From Induced Pluripotent Stem Cells With Long-QT Syndrome 3 Recapitulate Typical Disease-Specific Features In Vitro. Circ Res 2011;109(8):841–7.
31. Weber W, Lienhart C, Baba MDE, Grass RN, Kohler T, Muller R, *et al.* Magnet-guided transduction of mammalian cells and mice using engineered magnetic lentiviral particles. J Biotechnol. 2009;141(3–4):118–22.
32. Furlani EJ, Furlani EP. A model for predicting magnetic targeting of multifunctional particles in the microvasculature. J Magn Magn Mater. 2007;312(1):187–93.
33. David AE, Cole AJ, Chertok B, Park YS, Yang VC. A combined theoretical and *in vitro* modeling approach for predicting the magnetic capture and retention of magnetic nanoparticles *in vivo*. J Control Release. 2011;152(1):67–75.
34. Shimizu K, Ito A, Lee JK, Yoshida T, Miwa K, Ishiguro H, *et al.* Construction of multi-layered cardiomyocyte sheets using magnetite nanoparticles and magnetic force. Biotechnol Bioeng. 2007;96(4):803–9.
35. Akiyama H, Ito A, Sato M, Kawabe Y, Kamihira M. Construction of cardiac tissue rings using a magnetic tissue fabrication technique. Int J Mol Sci. 2010;11(8):2910–20.
36. Chorny M, Fishbein I, Yellen BB, Alferiev IS, Bakay M, Ganta S, *et al.* Targeting stents with local delivery of paclitaxel-loaded magnetic nanoparticles using uniform fields. Proc Natl Acad Sci U S A. 2010;107(18):8346–51.
37. Riegler J, Wells JA, Kyrtatos PG, Price AN, Pankhurst QA, Lythgoe MF. Targeted magnetic delivery and tracking of cells using a magnetic resonance imaging system. Biomaterials. 2010;31(20):5366–71.